OPEN ACCESS

International
Journal
Of Modern Engineering Research (IJMER)

Deep learning application for events classification of energy-dispersive Laue diffraction datasets collected by pnCCD

A. Tosson[1], D. Bahrami[1], A. Davtyan[1], M. Shokr[1] and U. Pietsch[1].
[1]*Faculty of Science and Engineering, University of Siegen, D-57068 Siegen, Germany*
Corresponding Author: A. Tosson

ABSTRACT:*Energy-dispersive Laue diffraction (EDLD) experiments represent a powerful and sophisticated technique for structural characterization of materials. The X-ray scattering, recorded by a 2D energy-dispersive detector, enables a full determination of the crystal structure. Operating the detector at ~ 600 - 1000Hz leads to a dramatic increase in the amount of collected data, which requiresmultiplesteps of preparatory analysis. Event classification and reconstruction are the instances of these steps, which have a huge impact on the final results. This paper introduces a deep learning module, based on a Convolution Neural Network (CNN), aimed at obtaining a fast and precise event classification. This module was trained ontwo datasets, namely the simulated and experimental samples, which resulted in outstanding performance: The final model has a precision of more than 99% in classifying EDLD events, compared to the results of standard evaluation procedures.*
KEY WORDS:*Deep learning, pnCCD, X-ray diffraction, Detectors*

Date of Submission:07-05-2019 Date of acceptance: 24-05-2019

I. INTRODUCTION

Nowadays, the third generation of high brilliance X-ray sources [1]iswidely used for different scientific applications, such as imaging, [2–4] astronomy, [5] medicine [6] and life science [7].With respect tothese applications, the use of reliable techniques in data handling, mining and processing has become a prerequisitefor asuccessful experiment. The fast developmentof the detector technology is one of the factors, which increasedconsiderably the volume of generated data. For example, the detectorscurrently used in the Large Hadron Collider (LHC) alone are recording 25 petabytes (25 million gigabytes) of data per year. Besides the LHC, the synchrotron radiation facilities around the world representanother source, generating a large volume of data in various scientific fields. In physics, X-ray crystallography (XRC) is a well-known toolfor determining the crystal structure, based on Bragg diffraction formed bynumerousatomic planes. One of XRCexperimental techniques to determine the crystal structure is the so-called Energy Dispersive Laue Diffraction (EDLD), which can be realized by using a white X-ray beam and a 2D energy-dispersive detector [8, 9].

The use offastreadout 2D detectors and polychromatic hard X-rays increases the amountof generated data, which may exceed tens of GByte/s [10]. Processing of large amounts of data on-the-fly is a challenging task, which requires multiple analyticalsteps (i.e. data streaming, data reconstruction, data mining and data interpretation) [11]. The conventional methodsof data treatment may lead to data loss and can be affected by complex aspectsofdata streaming, such as time efficiency, memory utilization and space occupancy [11]. Thus, many scientific researchers have adopted Deep Learning (DL) techniques tosolve the problems aboutimaging of straininnanocrystals [12]and classifying crystal structures as well as [13] Machine Learning (ML) techniques to resolve the issues about X-ray diffraction-based classification [14] and imaging of nanoscale lattice vibrations [15]. The idea behind the implementation of DL methods in data analysis is their enormouscomputational power to process massive datasets. [16] Furthermore, DL architectures have recently outperformed humans in visual tasks, namely object recognition and image classification [17].This paper presents a DL-based approach for data reconstruction ina Laue diffraction experiment with synchrotron radiation, using a white X-ray beam and an energy-dispersive 2D detector (pnCCD). This approach is able to classifythe patterns of single photons, hereinafter referred to as events, collected during EDLD experiments. The model aimed at performingthis task employs the Softmax [18] function at the classification layer. To predict a classification of patterns, a Convolutional Neural Network (CNN) [19] was built up. Thistypeof artificial neural networks, having multiple layers between an input and an output layers, is mostly applied to analyze visual images. To create thetraining

and validation datasets for the algorithm, more than 70000 events have been simulated and extracted under supervised classification.

II. PNCCD CONCEPT

The concept of pnCCD, as an energy-resolving area detector, is based on the principle of sideward depletion in high resistivity silicon. This basis allows for time resolution, simultaneous position measurement and energy dispersive detection of X-rays, with a low level of noise and a fast readout [20]. The system serves as a flexible large area detector in order both to resolve single photons in the spectroscopic operation mode and to count photons with a high dynamic range in the single photons counting mode. The pnCCD entrance window covers the area of 8.3 cm^2 with 384 x 384 pixels, where each pixel has a size of 75 x 75 μm^2.

When the system is operating in the single photons counting mode, only few photons are recorded and not more than one photon is triggered by one pixel during each frame time interval. The number of the generated electrons in the charge cloud depends on the energy of the absorbed photon. The charge cloud expands due tothe drift and diffusion of electrons, passing through the siliconwindow towards the front end. The final size of the charge cloud, at the pixel plane, depends on the photon energy and the absorption depth within the depleted silicon substrate. The photon impact is localized at one pixel (single), two (doubles), three (triples) or four (quadruples) pixels, depending on the relative position and the size of the generated cloud [21]. Singles, left and right doubles, up and down doubles, four types of triples and four types of quadruples result in 13 possible patterns, shown in figure 1. The patterns which cannot be described by one of these 13 types are obviously not created by a single-photon impact and are defined as fall-out events. Figure 2 shows examples of fall-out events recorded during an experiment.The dashed frames represent the borders of each event. Each event is a combination oftwo or more single-photon events shown in figure 1. Figures 2a and 2b display twofold events, while figures 2c and 2d show threefold combination. Fall-out events are denoted as"unknown events" and their contribution is neglected by conventional analytical tools. These events account for from15% to 40% of the total recorded events, depending on many factors, such as beam flux and frame-readout frequency. This impedes the determination of the actual number of photons detected during the experiment. As a result, the evaluated data set is incomplete and limits the outcome of subsequent data treatment, for example, for X-ray structure analysis [25]. Thus, many applications, demandingextremelyprecise calculations (i.e. structure factor analysis) are difficult to be performed due to involvement of multiple complex correction steps. Setting outto widen the range of pnCCDapplications, the issue of fall-out events has to be addressed.

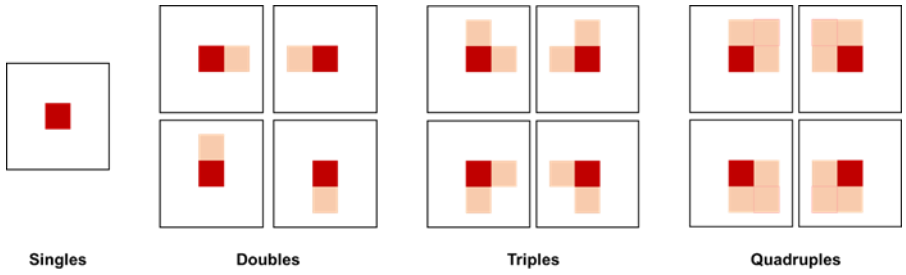

Figure 1: Thirteen possible event types originating from the interaction of single photon with pnCCD detector.

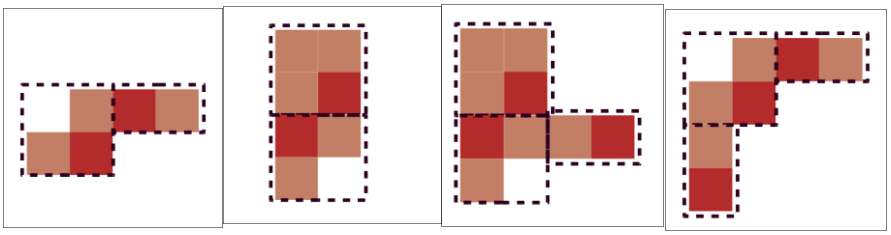

(a)Triple-double (b)Quadruple-triple (c)Triple-double-quadruple (d)Twodoubles-double

Figure 2: Examples offall-out events.

III. CLASSIFICATION AND RECONSTRUCTION OF EVENTS

Prior to further analysis of the EDLD experiment, the recorded raw event data illustratedin section 2 have to be reconstructed. This process is composed of two main steps:

. Classification of event patterns: the events are categorized according tofive types (single-pixel events, three classes of multi-pixel events and unknown events), as shown in figure 1.
. Reconstruction of events: the multi-pixel events are reconstructed to individual photon hits by determining the center-of-mass coordinates of each event.

Achieving real-time event reconstruction is a challenging task because of the huge volume of data collected during the experiment. A typical one-shot data set, taken by the single photon counting mode, contains 5 x 10^4 frames with ≈ 300 event/frame. However, the use of a traditional serial Application Programming Interface (API) induces high latency execution time and data loss [11]. Therefore, many studiesemployed the parallel processor technology and multi-core Graphic Processing Units (GPUs) in order to realize the in-situ reconstruction of events [11, 22, 23]. Although these approaches have proven to bea reliable technique inthe case of single-photon events reconstruction, they fail to offer a solution for fall-out events. The present paper introduces a state of art DL-based application to achieve a precise classification of patterns for single photon events. Furthermore, this approach serves as a seed for reconstruction of fall-out events.

The following sections are organized as follows: Section 4 describes theprocess of data preparation and outlines the training, validation and testing phases. Section 5 provides a summary of the network architecture used for this model. Section 6 illustrates the results of the analysis. Finally, section 7 provides the conclusion and addresses some open problems for further investigation.

IV. TRAINING, VALIDATION AND TESTING PHASES

In order to assure the quality of the training procedure, two datasets were used in combination: namely the simulated and experimental samples. The simulated dataset was generated based on constraints and conditions defined by a typical EDLD experiment, including all permutations of the events. Since the detector size is 384 x 384 pixels, a single frame image is, in fact, a sparse matrix with only few events. To avoid large sparsity, 9 x 9 pixel window was used to cut out single, double, triple or quadruple events, as shown in figure 3. In this manner, a dataset comprising52000 events was simulated, with the events randomly distributed across different x,y pixel positions on the detector. The experimental dataset consists of more than 18000 labeled events, collected from different experiments which were performed using different X-ray facilities (i.e. DELTA, EDDI, ESRF…etc.). The simulated and experimental datasets were used to feed the module during the training-validation phase, after combining and shuffling them.

Totest the response of the trained module, only labeled experimental datasets from several experimental setups were utilized. This allows ensuringthe reliability of the module for any experimental data, regardless of the experimental conditions.

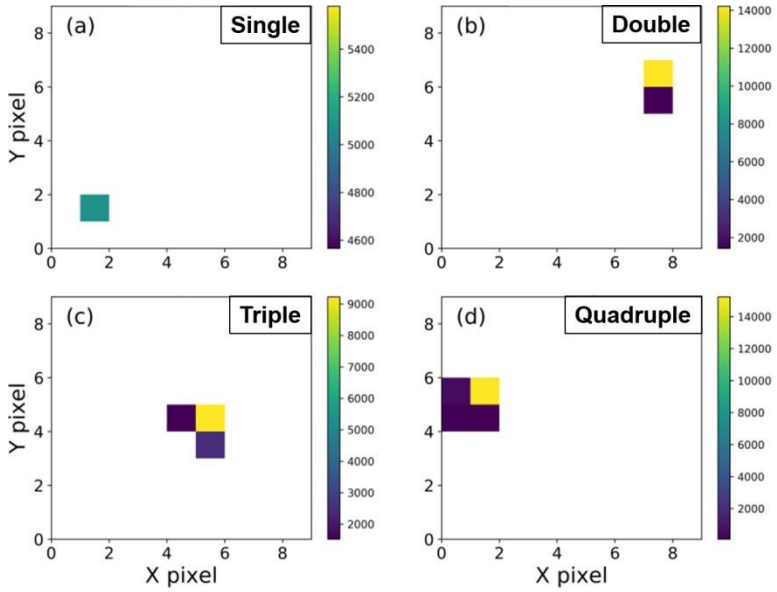

Figure 3: Randomly chosen events from the simulated dataset. Single, double, triple and quadruple events are shown correspondingly in a,b,c, and d.

V. NETWORK ARCHITECTURE

The events classifying architecture is shown in figure 4. It is composed of an input layer, followed by three 2D- convolutional (Conv2D) layers with rectified linear unit (ReLu) activation function, each of whichis connected with a maximizing pooling layer. The output of these layers is flattened and sent to a fully connected

layer with Softmax activation function. Anoutput layer contains five classes. In order to boost the performance of the CNN, the ReLu is coupled with dropout that has a rate of 35%.

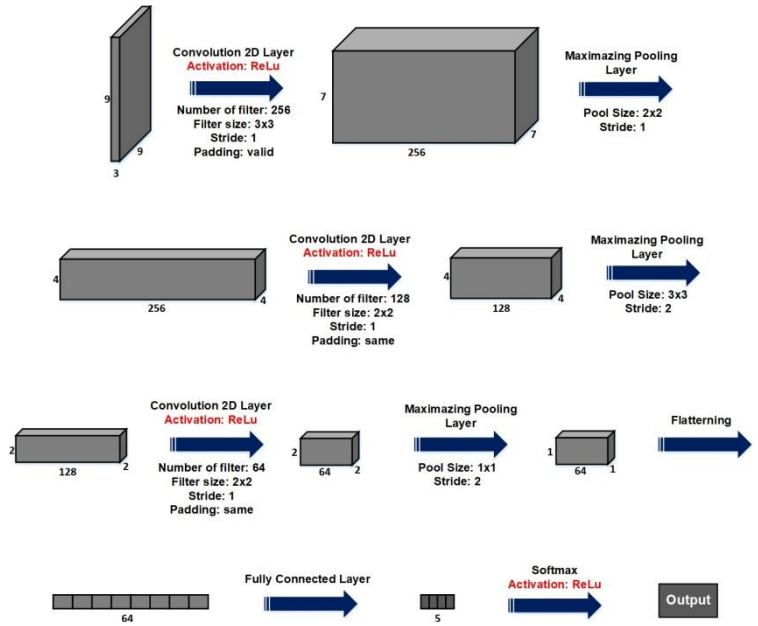

Figure 4: The convolutional neural network (CNN), containing an input layer, three pairs of convolutional and pooling layers, a fully connected layer and an output layer.

The hyper-parameters (i.e. the numbers of layers, the number of neurons in each layer, the size and number offilters, the stride size, the rate of dropout, the learning rate, the optimizer...etc.) have been selected by trial and error method, after extensivetestsof the performance of numerous architecture versions.

The events image data arestreamed as a 3D sparse-matrix, with 9 x 9 x 3 elements representing the X, Y sizes and 3 RGB-channels for each element respectively. The images are streamed as patches to the network, producingan output as probabilities of one of the five classes indicating the event type (single, double, triple, quadruple or unknown). The features of Keras library with TensorFlow back-end have been implemented for the network design. The data were split into two sets, i.e. the training set and the validation set, with splitting ratio of (90 - 10%). The training phase was executed using a machine with specifications provided in table 1. The network filter coefficients have been trained using the sparse-categorical cross-entropy loss function optimization with a learning-rate of 0.001. Adam optimizer has been utilizedto improve efficiency ofthe cost function with the default values offered by the author, namely $\beta1 = 0.9$, $\beta2 = 0.999$ and $s = 10^{-8}$[24]. The model was fitted with 30 (see figures 5a and 5b) and 100 (see figures 5c and 5d) epochs, with the patch size of 128. The accuracy and loss curves for different number of epochs are presented in figure. 5. As shown in both modules, the weights converge within the first 30 epochs follow exponential decay function. Figure 5d displays linear converge behavior between 30 and 100 epochs. After more than 100 epochs, the validation loss starts diverging;this is an indication of over-fitting. Thus, a decision was taken to set100 epochs as the maximum value for training-validation phase. Figure 6 shows the summary of the layers and the parameters. At the end of the training-validation phase, two trained-modules have been generated for the testing phase, namely Events-Classifier30 and Events-Classifier100.

Table 1: Specifications of the system employed.

Feature	Specification
Model	Dell Latitude 5480
Processor	Intel Core i7-7600U
Speed	2.8GHz(4 CPU)
GPU	Nvidia GeForce 930MX

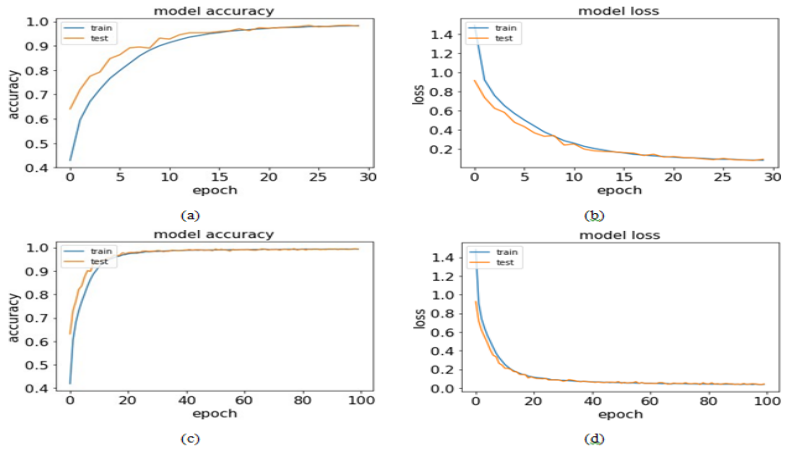

Figure 5: The accuracy and loss curves. (a) and (b) are for 30 epochs, while (c) and (d) are for 100 epochs. The blue and orange lines are corresponding to the training and the validation phases respectively.

VI. RESULTS

The two trained-modules have been tested with the same testing datasets. The prediction accuracy has been calculated, as follows:

$$\text{Predictionaccuracy}\% = \frac{\text{Total number of the correctly predicted events}}{\text{Total numberofevents}} \times 100$$

The module Events-Classifier30 shows the average prediction accuracy of≈ 92%, while the module Events-Classifier100 is able to reach more than 99% of the prediction accuracy relative to conventional evaluation tools. As a result, the CNN correctly predicts the events patterns and categorizes the streamed events in five different classes, namely single, double, triple, quadruple and fall-out events. Allinall, Events-Classifier100 providesa reliable approach that can be used for further implementation. Both models give execution time of 3.9 ± 0.03 sec per 5×10^4event (≈ 167 frame). However, this time is quite long compared with the current method which can perform the same data size in 1.1 ± 0.1 sec [11].

Layer (type)	Output Shape	Param #
conv2d (Conv2D)	(None, 7, 7, 256)	7168
activation (Activation)	(None, 7, 7, 256)	0
dropout (Dropout)	(None, 7, 7, 256)	0
max_pooling2d (MaxPooling2D)	(None, 4, 4, 256)	0
conv2d_1 (Conv2D)	(None, 4, 4, 256)	262400
activation_1 (Activation)	(None, 4, 4, 256)	0
dropout_1 (Dropout)	(None, 4, 4, 256)	0
max_pooling2d_1 (MaxPooling2	(None, 2, 2, 256)	0
conv2d_2 (Conv2D)	(None, 2, 2, 256)	262400
activation_2 (Activation)	(None, 2, 2, 256)	0
dropout_2 (Dropout)	(None, 2, 2, 256)	0
max_pooling2d_2 (MaxPooling2	(None, 1, 1, 256)	0
flatten (Flatten)	(None, 256)	0
dense (Dense)	(None, 64)	16448
dense_1 (Dense)	(None, 5)	325
activation_3 (Activation)	(None, 5)	0

Total params: 548,741
Trainable params: 548,741
Non-trainable params: 0

Figure 6: Layers and parameters of the network architecture.

VII. CONCLUSION AND OUTLOOK

This paper hasdemonstrated how DL-basedalgorithmscould be applied for event classification. The module, consisting of a multi-layer CNN,was trained onthe simulated and experimental datasets to extract the information enabling the prediction of event patterns. The testing phase, which was performed using theexperimental datasets, shows the model's prediction accuracy up to 99%.

As a next step, the DL-based approach will be extended to include the analysis of fall-out events. The focus will also be on the optimization of execution time to achieve a full classification of events in real-time.

VIII. AKNOWLEDGMENT

This research was supported byBundesministerium für Bildung und Forschung. We thank our colleagues from computer science department, Siegen University, who provided insight and expertise that greatly assisted the research. We would also like to show our gratitude to L.Strüder and R. Hartmann, PNSensor GmbH, for their technical support. We are also immensely grateful to V. Pankova, Bonn University for her comments that greatly improved the manuscript.

REFERENCES

[1]. Namkung, W., "Review of third generation light sources," Int. Particle Accelerator Conf., Kyoto,Japan
[2]. (2010).
[3]. Logan, C. M., Schneberk, D. J., Shull, P. J., and Martz, H. E., [X-ray Imaging: fundamentals, industrial techniques and applications], CRC Press(2016).
[4]. Davtyan, A., Krause, T., Kriegner, D., Al-Hassan, A., Bahrami, D., Mostafavi Kashani, S. M.,Lewis,
[5]. R.B.,Küpers,H.,Tahraoui,A.,Geelhaar,L., et al.,"Threefoldrotationalsymmetryinhexagonallyshaped core–shell (in, ga) as/gaas nanowires revealed by coherent x-ray diffraction imaging," Journal of applied crystallography 50(3), 673–680 (2017).
[6]. Maddali, S.,Calvo-AlmazanI., AlmerJ., KeneseiP., ParkJ.-S., HarderR., Nashed Y.&HruszkewyczS. O.,"Sparse recovery of undersampled intensity patterns for coherent diffraction imaging at high X-ray energies"Scientific Reports 84959(2018).
[7]. DePasquale, J., Arcand, K., and Edmonds, P., "High energy vision: Processing x-rays," arXiv preprint arXiv:1509.07753(2015).
[8]. Roobottom,C.,Mitchell,G.,andMorgan-Hughes,G.,"Radiation-reductionstrategiesincardiaccomputed tomographicangiography,"Clinicalradiology65(11),859–867(2010).
[9]. Sayers,Z.,Avşar,B.,Cholak,E.,andKarmous,I.,"Applicationofadvancedx-raymethodsinlifesciences,"
[10]. BiochimicaetBiophysicaActa (BBA)-General Subjects 1861(1), 3671–3685 (2017).
[11]. Hajdu,J.,Machin,P.A.,Campbell,J.W.,Greenhough,T.J.,Clifton,I.J.,Zurek,S.,Gover,S.,Johnson,
[12]. L.N.,andElder,M.,"Millisecondx-raydiffractionandthefirstelectrondensitymapfromlauephotographs ofaproteincrystal,"Nature329(6135),178(1987).
[13]. Leitenberger,W.,Hartmann,R.,Pietsch,U., Andritschke,R.,Starke,I.,andStrüder,L.,"Applicationof a pnccd in x-ray diffraction: a three-dimensional x-ray detector," Journal of Synchrotron Radiation 15(5), 449–457(2008).
[14]. Bicer, T., "Real-time data analysis and autonomous steering of synchrotron light source experiments,"13th IEEEInternationalConferenceoneScience,Auckland,NewZealand(2017).
[15]. Tosson,A.,Shokr,M.,Abboud,A.,Bebawy,Y.,Algashi,A.,Hartmann,R.,Klaus,M.,Genzel,C.,Strüder, L., and Pietsch, U., "Edld-tool: A real-time gpu-based tool to stream and analyze energy-dispersive laue diffractionofbigdatasetscollectedbyapnccd,"JournalofInstrumentation14(01),P01008(2019).
[16]. Cherukara, M. J., Nashed, Y. S., and Harder, R. J., "Real-time coherent diffraction inversion using deep generative networks," Scientific reports8(1), 16520 (2018).
[17]. Park, W. B., Chung, J., Jung, J., Sohn, K., Singh, S. P., Pyo, M., Shin, N., and Sohn, K.-S., "Classification ofcrystalstructureusingaconvolutionalneuralnetwork,"IUCrJ4(4),486–494(2017).
[18]. Zhao, B., Wolter, S., and Greenberg, J. A., "Application of machine learning to x-ray diffraction-based classification," in [Anomaly Detection and Imaging with X-Rays (ADIX) III], 10632, 1063205, International SocietyforOpticsandPhotonics(2018).
[19]. Laanait,N.,Zhang,Z.,andSchlepütz,C.M.,"Imagingnanoscalelatticevariationsbymachinelearningof x-raydiffractionmicroscopydata,"Nanotechnology27(37),374002(2016).
[20]. LeCun,Y.,Bengio,Y.,andHinton,G.,"Deeplearning,"Nature521,436–44(052015).
[21]. Esteva, Andre Kuprel, B. N. R. A. K. J. S. S. M. B. H. M. T. S., "Dermatologist-level classification of skin cancerwithdeepneuralnetworks,"Nature542(1)(2017).
[22]. Gao, B. and Pavel, L., "On the properties of the softmax function with application in game theory and reinforcement learning," (042017).
[23]. TianyiLiu,ShuangsangFang,Y.Z.P.W.J.Z.,"Implementationoftrainingconvolutionalneuralnetworks," (062015).
[24]. Andritschke, R., Hartner, G., Hartmann, R., Meidinger, N., and Struder, L., "Data analysis for character- izingpnccds," in [2008 IEEE Nuclear Science Symposium Conference Record], 2166–2172, IEEE(2008).
[25]. Abboud,A.,Send,S.,Pashniak,N.,Leitenberger,W.,Ihle,S.,Huth,M.,Hartmann,R.,Strüder,L.,and Pietsch, U., "Sub-pixel resolution of a pnccd for x-ray white beam applications," Journal of Instrumenta- tion 8(05), P05005 (2013).
[26]. F. Alghabi, S. Send, U. S. A. A. U. P. and Kolb, A., "Fast gpu-based absolute intensity determination for energy-dispersive x-ray laue diffraction,," Ltd and SissaMedialabsrl (2016).
[27]. F. Alghabi, S. Send, U. S. A. A. U. P. and Kolb, A., "Fast gpu-based spot extraction for energy-dispersive x-ray laue diffraction," Journal of Instrumentation 9 (2014).
[28]. Kingma, D. P. and Ba, J., "Adam: A method for stochastic optimization," arXiv preprint arXiv:1412.6980(2014).
[29]. Send, Sebastian, et al. "Application of a pnCCD for energy-dispersive Laue diffraction with ultra-hard X-rays." Journal of Applied Crystallography 49.1 (2016): 222-233.

A. Tosson" Deep learning application for events classification of energy-dispersive Laue diffraction datasets collected by pnCCD" International Journal of Modern Engineering Research (IJMER), vol. 09, no. 3, 2019, pp 01-06